Supplementary Information

Structural and Electronic Transition of layered $PtSe_2$ into non-layered PtSe

Kuanysh Zhussupbekov[1,2,3,,†], Samuel Berman[1,†], Maximilian Prechtl[4], Marc Busch[4], Ainur Zhussupbekova[1,2], Georg S. Duesberg[4], Valeria Nicolosi[2], Kostya S. Novoselov[5,6] Cormac Ó Coileáin[4,#] and Igor V. Shvets[1,§]*

[1] School of Physics, Trinity College Dublin, Dublin 2, D02 PN40, Ireland

[2] School of Chemistry, Trinity College Dublin, Dublin 2, D02 PN40, Ireland

[3] Kh. Dosmukhamedov Atyrau University, Studenchesky Ave.,1, Atyrau, Kazakhstan

[4] Institute of Physics, EIT 2, Faculty of Electrical Engineering and Information Technology & SENS Research Center, University of the Bundeswehr Munich

[5] Institute for Functional Intelligent Materials, National University of Singapore, 4 Science Drive 2, 117544, Singapore

[6] National Graphene Institute, University of Manchester, Oxford Road, Manchester, M13 9PL, United Kingdom

1. XPS/XRD/XRR measurements

X-ray diffraction (XRD) and XPS, Figures S1(a-f), were utilised to confirm the successful synthesis of the $PtSe_2$ films and assess changes in the films after UHV annealing. XPS was performed to investigate the compositional quality and the VB region of the CVD grown $PtSe_2$ films before and after UHV annealing. Figures SI1(a, b) display the spectra of the Se 3*d* and Pt 4*f* core-level areas of the initial $PtSe_2$. Energies were corrected with respect to C1*s* 284.8 eV. The Pt 4*f* core-level spectrum is composed of four significant contributions: a main doublet peak at ~ 73.7 eV ($4f_{7/2}$), indicating 71% bound as Pt-Se_2, another smaller doublet at ~ 73.1 eV ($4f_{7/2}$), indicating 21% bound as Pt-Se, and the smaller peaks positioned at ~ 75.2 eV (7%) and 71.8 eV (2%), can be attributed to Pt-oxides and unreacted Pt metal, respectively.[1] Thus the majority of the Pt is bound to Se, but some oxides and elemental Pt are present. This is in line with previous XPS reports on $PtSe_2$.[2] The Se 3*d* core-level spectrum is deconvoluted into two contributions: Se-Pt dominates at 54.9 eV (the expected energy separation between Pt-Se_2 and Pt-Se is too small for the contributions to be separately distinguished) and the other comparatively minor contribution at 58.1 eV is probably indicative of Se-O/amorphous Se.[3]

XRD was used to evaluate the crystallinity of the $PtSe_2$ film prior to (blue) and after (red) thermal treatment in UHV at 500 °C for 4 hours to produce PtSe (see Figure SI1(c-e)).[4] From the XRD pattern, it is clear that the main characteristic peak of $PtSe_2$ (001), at 17.29°, disappears after thermal treatment, while the secondary peaks at 40.621° and 45.18° broaden and display reduced intensity, indicating increased disorder.[5] The strong peak at 69° originates from the Si substrate.

Figure 1(f) shows the measured valance band XPS of the samples with $PtSe_2$ and PtSe (solid spectra) alongside the DFT calculated density of states (DOS) for $PtSe_2$ and PtSe slabs (dashed spectra). XPS measurements of the VB demonstrate that the DOS near the Fermi level (FL) increases after annealing at 500 °C for 4 hours (red curve). After the UHV heating the film appears to exhibit more pronounced metallic properties. Our DFT calculations of the fully relaxed $PtSe_2$ and PtSe are in good agreement with the experiment. The increased DOS at the FL for PtSe vs $PtSe_2$ is captured, and the overall shape of the DOS curves is largely in agreement with the increases observed the measured spectra. In the PtSe structure, the pronounced DOS near the FL mainly arises from the 5d electrons of the Pt, which demonstrate metallic properties (see Figure SI3).

From the XPS studies, it can be concluded that annealing causes a loss of Se, and DFT suggests the formation of PtSe with a tetragonal lattice and metallic properties. This process leads to a change in the spectrum of electronic states: the proportion of Se compared to Pt decreases, which leads to the evolution in the VB XPS spectra near the FL in Figure SI1(f).

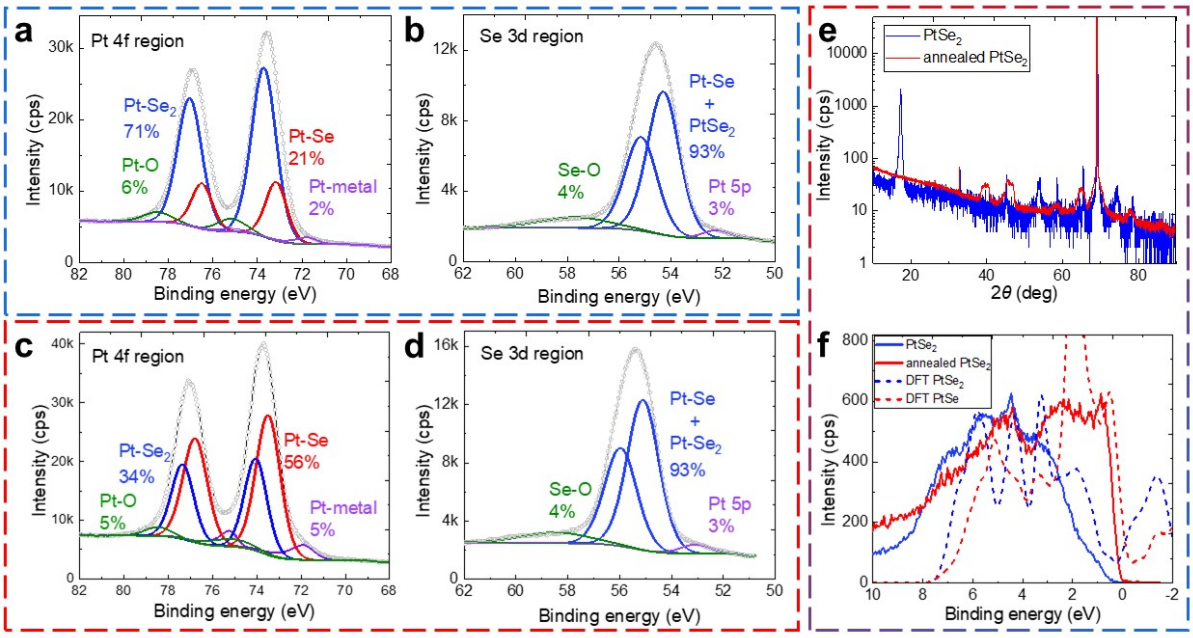

Figure SI1. CVD grown polycrystalline $PtSe_2$ films before and after annealing. XPS of $PtSe_2$ film showing the Pt 4f (a) and Se 3d (b) core levels prior to annealing. (c) and (d) XPS spectra of Pt 4f and Se 3d core levels after an annealing series to 500 °C for 1 hour. (e) XRD of $PtSe_2$ film before and after UHV heating at 500 °C for 4 hours, displaying characteristic $PtSe_2$ peaks and a peak at 69° from the Si substrate. (f) Experimental VB XPS of the $PtSe_2$ film before and after UHV annealing at 500 °C for 4 hours and calculated VB states of the $PtSe_2$ and PtSe

X-ray reflection (XRR) patterns generated from $PtSe_2$ film before any treatment and after UHV annealing at 500 °C are shown in Figure SI2. The thickness (d), density (ρ) and roughness (rms) are determined from the fitting of Kiessig fringes and critical point in the LEPTOS software. Annealing of the film resulted in a reduction in the thickness, from 23 to nm 20 nm, and a change in density of the films, supporting the conclusion that the transformation that occurred. The complete reduction of the film to Pt can be effectively ruled out as greater loss would be expected. However, roughness (RMS) of the film is increased from ~1.2 nm to ~4.5 nm after the annealing procedure. The density is also apparently reduced after annealing, which in combination with the reduced thickness is consistent with reduced mass with due to Se loss when transitioning to PtSe.

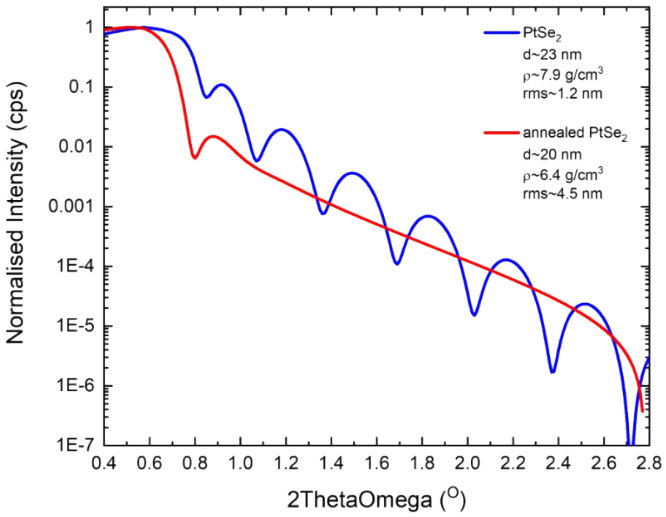

Figure SI2. XRR of the $PtSe_2$ prior and after annealing in UHV at 500 °C.

2. Orbital projected DOS

Figure SI3 presents the orbital projected density of states (DOS) for fully relaxed structures of both $PtSe_2$ (a) and PtSe (b). The scales in (a) and (b) are the same for better comparison. It is apparent that states next to Fermi level in the PtSe are mostly contributed by the Pt 5d electrons (green).

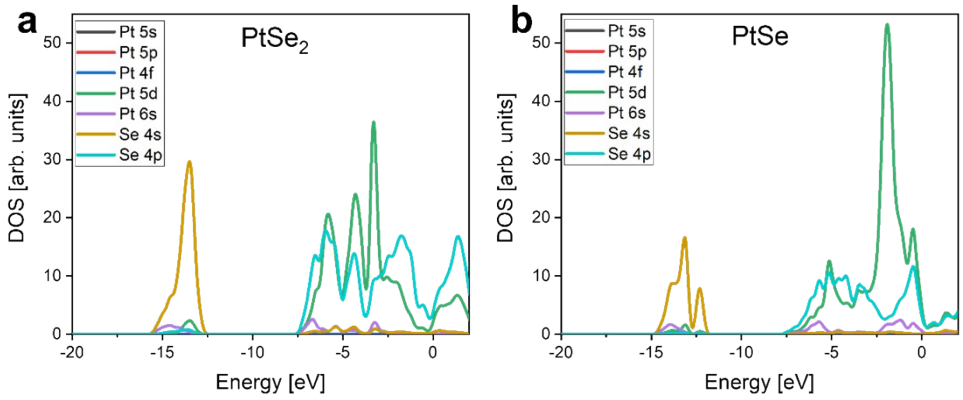

Figure SI3. Orbital projected DOS for the $PtSe_2$ and PtSe (a) Orbital projected DOS calculation of the $PtSe_2$ structure. **(b)** Orbital projected DOS calculation of the PtSe.

3. STM line profiles

Figure SI4(a) and Figure SI4(c) are larger area STM images of the $PtSe_2$ and PtSe films, respectively, showing the crystallites where the high resolution STM and STS measurements were performed. Figure SI4(b) and Figure SI4(d) are the line profiles indicated in the STM

images of $PtSe_2$ (Figure SI4(a)) and PtSe (Figure SI4(c)) demonstrating the nominal thicknesses of each crystallite.

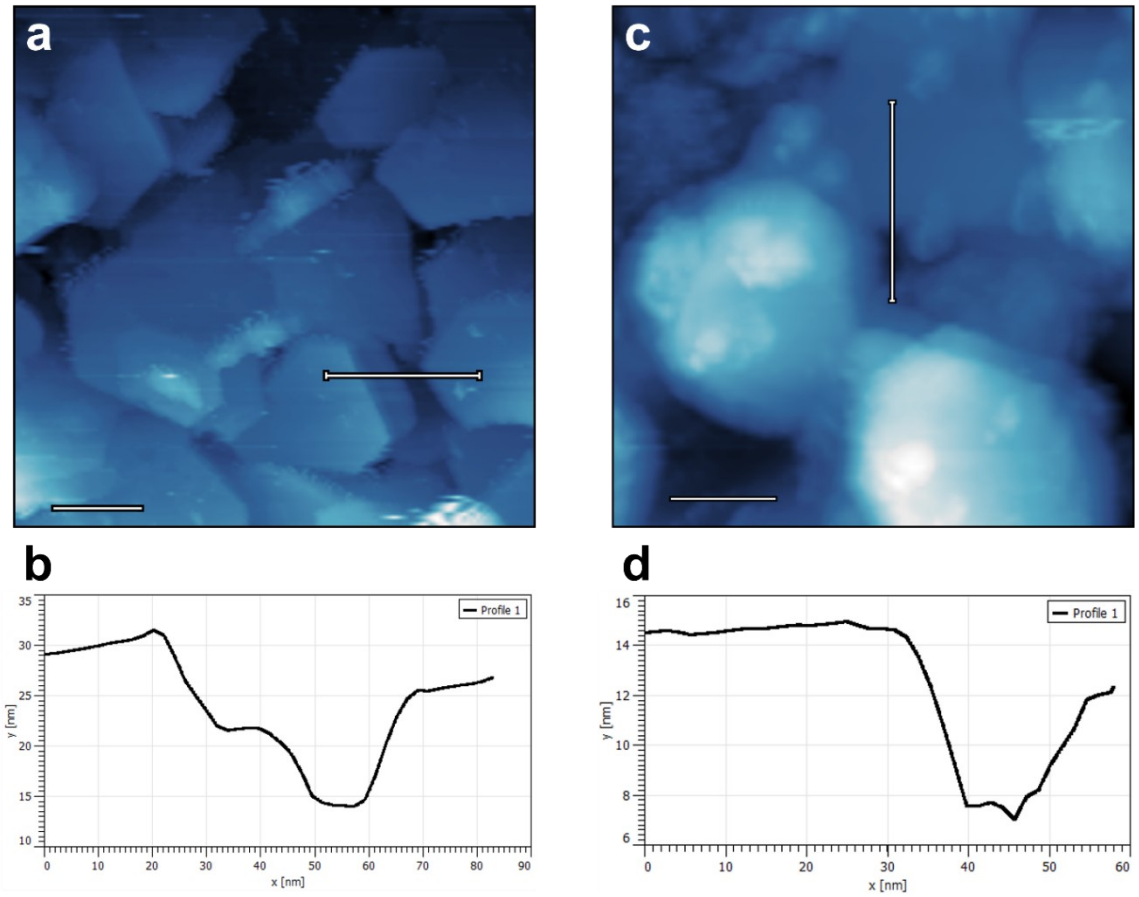

Figure SI4. STM images of the $PtSe_2$ and PtSe with line profiles. (a) Large area STM topography of CVD-grown $PtSe_2$ film (250×250 nm^2, I=1.5 nA, V=2.8 V, RMS=7.120 nm). **(b)** The line profile of the $PtSe_2$ flake (around 19 nm at least) where STM and STS measurements were performed. **(c)** STM topography of PtSe film (150 × 150 nm^2, V = 2.0 V and I = 500 pA). **(d)** The line profile of the PtSe film demonstrating that PtSe crystallite is at least 8 nm thick.

REFERENCES

1. Yim, C., et al., *High-Performance Hybrid Electronic Devices from Layered PtSe2 Films Grown at Low Temperature.* Acs Nano, 2016. **10**(10): p. 9550-9558.
2. Jiang, W., et al., *Large-area high quality PtSe2 thin film with versatile polarity.* Infomat, 2019. **1**(2): p. 260-267.
3. Wang, G.Z., et al., *Ultrafast Carrier Dynamics and Bandgap Renormalization in Layered PtSe2.* Small, 2019. **15**(34): p. 9.
4. Gronvold, F., H. Haraldsen, and A. Kjekshus, *On the Sulfides, Selenides and Tellurides of Platinum.* Acta Chemica Scandinavica, 1960. **14**(9): p. 1879-1893.
5. Zeng, L.H., et al., *Ultrafast and sensitive photodetector based on a PtSe2/silicon nanowire array heterojunction with a multiband spectral response from 200 to 1550 nm.* Npg Asia Materials, 2018. **10**: p. 352-362.